Algorithms for digital image processing in diabetic retinopathy

R.J. Winder [a,*], P.J. Morrow [b], I.N. McRitchie [a], J.R. Bailie [c], P.M. Hart [d]

[a] Health and Rehabilitation Sciences Research Institute, University of Ulster, Shore Road, Newtownabbey BT37 0QB, United Kingdom
[b] School of Computing and Information Engineering, University of Ulster, Cromore Road, Coleraine BT52 1SA, United Kingdom
[c] Health and Social Care Research and Development Office, 12 – 22 Linenhall Street, Belfast BT2 8BS, United Kingdom
[d] Northern Ireland Diabetic Retinopathy Screening Service, Belfast Health and Social Care Trust, Royal Group of Hospitals, Grosvenor Road, Belfast BT12 6BA, United Kingdom

ARTICLE INFO

ABSTRACT

This work examined recent literature on digital image processing in the field of diabetic retinopathy. Algorithms were categorized into 5 steps (preprocessing; localization and segmentation of the optic disk; segmentation of the retinal vasculature; localization of the macula and fovea; localization and segmentation of retinopathy). The variety of outcome measures, use of a gold standard or ground truth, data sample sizes and the use of image databases is discussed. It is intended that our classification of algorithms into a small number of categories, definition of terms and discussion of evolving techniques will provide guidance to algorithm designers for diabetic retinopathy.

© 2009 Elsevier Ltd. All rights reserved.

1. Introduction

Over the last decade, high resolution color digital photography has been recognized as an acceptable modality for documenting retinal appearance. Images are easily captured using a conventional digital camera back, attached to a retinal camera body designed to compensate for the optics of the eye. The digital format provides a permanent, high quality record of the appearance of the retina at any point in time. Electronic storage, retrieval and transmission are possible without loss of image quality.

One well recognized application for retinal digital imaging is within screening programs for diabetic retinopathy (DR). This disease is the commonest cause of blindness in people of working age, has an effective treatment available to prevent vision loss but is asymptomatic until late in the disease process. The UK National Screening Committee currently recommends annual screening for all diabetic patients aged 12 years and over, using digital retinal photography (www.nscretinopathy.org.uk). Images may be captured at a venue convenient to the patient's home or work and data then transferred to a central location where they are read and interpreted by trained graders. Quality assurance must be an integral component of any screening programme, and as in breast screening programs, a high proportion of all images should be double read.

Population growth, an aging population, physical inactivity and increasing levels of obesity are contributing factors to the increase in the prevalence of diabetes. The global prevalence of diabetes is expected to rise from 2.8% in 2000 to 4.4% of the global population by 2030 [1]. In the UK the number of diabetic people is approximately 2.3 million (www.diabetes.org.uk). If all diabetic people are to undergo regular screening within a quality assured framework, the workload is going to be substantial.

Grading retinal images for the presence of diabetic retinopathy is largely a pattern recognition task. The typical features of diabetic retinopathy are microaneurysms, small intra retinal dot hemorrhages, larger blot hemorrhages, all of which are red lesions, and whitish lesions for example lipid exudates, and cotton wool spots which are nerve fiber layer microinfarcts. Graders are taught to recognize these lesions against the background appearance of the 'normal retina'. With an increasing diabetic population and the need for quality assurance pathways, it is not surprising that considerable effort has been spent over the past 10–15 years on investigating whether these lesions could be detected by computer aided pattern recognition algorithms.

The process of detecting multiple patterns and their relationship within a retinal image is made up of a series of operations or steps, with low-level image processing operations providing a basis for higher level analysis. Digital retinal images are usually processed in an algorithmic sequence, with the output of one stage forming the input to the next. For example, a typical sequence may consist of one or more preprocessing procedures followed by image segmentation, feature extraction and classification stages. Preprocessing may be used to normalize image brightness, correct for image non-uniformity, reduce noise or reduce image artifacts. Segmentation decomposes an image into its constituent regions or objects, for example retinal blood vessels, optic nerve head or pathological lesions. Feature extraction typically computes quantitative infor-

* Corresponding author. Tel.: +44 2890368440; fax: +44 2890368068.
E-mail address: rj.winder@ulster.ac.uk (R.J. Winder).

Table 1
List of references of the papers which addressed steps A–E either in part or in full.

A. Preprocessing
  Badea et al. [78]; Cree et al. [25]; Ege et al. [37]; Foracchia et al. [6]; Gagnon et al. [96]; Goatman et al. [23]; Goh et al. [103]; Hipwell et al. [68]; Narasimha-Iyer et al. [126,64]; Osareh et al. [24]; Raman et al. [139]; Sinthanayothin et al [71,145]; Usher et al. [27]; Walter and Klein [152]; Yang et al. [157]; Zhang and Chutatape [158]

B. Localization and segmentation of the optic disk
  Abdel-Razik et al. [76]; Chutatape and Li [86]; Eswaran et al. [92]; Fleming et al. [94]; Foracchia et al. [8]; Gagnon et al. [96]; Goh et al. [103]; Hajer et al. [106]; Hoover and Goldbaum [43,3]; Hwee et al. [112]; Kochner et al. [36]; Lalonde et al. [41]; Lee et al. [118]; Li and Chutatape [120,121,63,39]; Lowell et al. [28]; Mendels et al. [49]; Narasimha-Iyer et al. [126,64]; Niemeijer et al. [130], Noronha et al. [132]; Osareh et al. [133]; Sanchez et al. [40]; Saradhi et al. [142]; Sekhar et al. [144]; Simandjuntak et al. [146]; Sinthanayothin et al. [21,71,145]; Tobin et al. [65]; Usher et al. [27]; Walter and Klein [46,13,152,153]

C. Segmentation of the retinal vasculature
  Abdel-Razik et al. [76]; Abdurrazaq et al. [77]; Can et al. [79,80,81]; Chanwimaluang et al. [82,83]; Chapman et al. [84]; Chutatape et al. [85,86]; Cornforth et al. [87]; Dua et al. [89]; Estabridis et al. [91]; Fang et al. [93]; Fleming et al. [94]; Gagnon et al. [96]; Gang et al. [97]; Gao et al. [99,100,101]; Goh et al. [103]; Grisan et al. [104]; Hayashi et al. [108]; Hong et al. [109,110]; Hoover et al. [44]; Hsu et al. [111]; Hwee et al. [112]; Iqbal et al. [113]; Jiang et al. [114]; Kochner et al. [36]; Lalonde et al. [30,117]; Leandro et al. [18]; Lee et al. [119]; Li and Chutatape [120,122]; Lowell et al. [53]; Mahadevan et al. [124]; Martinez-Perez et al. [125]; Narasimha-Iyer et al. [126,64]; Niemeijer et al. [131,129]; Noronha et al. [132]; Pedersen et al. [135]; Pham et al. [136]; Raman et al. [139]; Sanchez et al. [40]; Simandjuntak et al. [146]; Sinthanayothin et al. [21,71,145]; Staal et al. [147]; Tan et al. [148]; Truitt et al. [149]; Tsai et al. [150]; Usher et al. [27]; Walter and Klein [46,13,152]; Yang et al. [57]

D. Localization of the macula and fovea
  Chutatape and Li [86]; Estabridis et al. [90]; Fleming et al. [94]; Gagnon et al. [96]; Li et al. [63,39]; Narasimha-Iyer et al. [126,64]; Niemeijer et al. [129]; Noronha et al. [132]; Simandjuntak et al. [146], Sinthanayothin et al. [21,71,145]; Tobin et al. [65]

E. Segmentation of retinopathy
  Badea et al. [78]; Cree et al. [25]; David et al. [88]; Ege et al. [37]; Estabridis et al. [90]; Eswaran et al. [92]; Fleming et al. [94]; Fleming et al. [95]; Gang et al. [98]; Garcia et al. [102]; Goh et al. [103]; Grisan et al. [105]; Hansen et al. [107]; Hipwell et al. [68]; Hsu et al. [111]; Kahai et al. [115,116]; Kochner et al. [36]; Larsen et al. [73]; Lee et al. [72]; Li et al. [120,63,39]; Luo et al. [123]; Narasimha-Iyer et al. [126,64]; Nayak et al. [127]; Niemeijer et al. [128,129]; Noronha et al. [132]; Osareh et al. [24]; Pallawala et al. [134]; Quellec et al. [137,138]; Raman et al. [139], Sagar et al. [140]; Sanchez et al. [40,141]; Satyarthi et al. [143]; Sinthanayothin et al. [71,145]; Truitt et al. [149]; Usher et al. [27]; Vallabha et al. [151]; Walter and Klein [13,152,153,154]; Wang et al. [14]; Xiaohui et al. [155,156]; Yang et al. [57,157]; Zhang and Chutatape [158]

mation from the segmented objects. The extracted features can be used to classify objects according to predetermined criteria such as size, morphology and color.

The objectives of this paper are

(1) to review the relevant literature over a 10 year period in the field of digital image processing in DR;
(2) to provide researchers with a detailed resource of the main algorithms employed;
(3) to categorize the literature into a series of operations or steps;
(4) to identify potential areas for improving research design and reporting.

The paper is organized as follows: Section 2 describes the methodology used for the literature review. Section 3 gives the results of the review. Section 4 provides a detailed survey of the common computational steps for detecting retinal features. The image processing operations for detecting the optic nerve head, retinal vasculature, fovea, macula and retinopathy are described. We conclude in Section 2 by discussing recent trends and directions for future work.

2. Literature survey methodology

In their 2003 report for NHS Health Technology Assessment (HTA) [2] Sharp and co-authors included in their objectives, a systematic literature review of digital imaging technology as applied to diabetic retinopathy. This review was completed in 1998. The authors stated that their original intent was to provide a quantitative analysis of different digital imaging techniques. They found that this was not possible owing to the early stage of evolution of digital technology in this field.

The work reported in this paper analyses and categorizes the literature on the use of digital imaging techniques in diabetic retinopathy during the period 1998–2008. Further literature is included in the text to illustrate the development of image processing techniques and algorithms in this field. However this supporting literature was not included in the analysis reported in Section 3. A survey methodology was developed which included the search

strategy, data extraction from the literature and analysis of findings. The following bibliographic databases were searched systematically: PubMed (National Library of Medicine), MEDLINE, EMBASE (Elsevier Science Publishers), Cochrane Library (Wiley), EI Compendex Plus (Elsevier Science Publishers); National Research Register (NRR), IEEExplore Digital Library (IEEE).

The studies included in this survey examined the use of novel computer algorithms to detect normal and pathological retinal features within the context of diabetic retinopathy. Secondary source articles describing the algorithms applied were identified from the reference lists of the reviewed articles and, although some were outside the date range, they were included for completeness. Analysis of the literature was carried out as follows: papers were categorized according to the image processing step(s) addressed and algorithms used; an analysis of reporting and/or evaluation methodologies was performed using the following five factors: reproducible description of the methodology; sample size if quoted; the use of a defined standard; objective result presented in numerical terms; sensitivity and specificity data reported. The literature was reviewed and a detailed overview of the image processing steps is presented in Section 4.

3. Literature survey results

One hundred and twenty seven articles were identified which met the criteria for inclusion. Where possible the main focus of each paper was identified, in terms of which step in the processing sequence was addressed. Five primary steps were defined: preprocessing (A); localization and segmentation of the optic disk (B); segmentation of the retinal vasculature (C); localization of the macula and fovea (D); and localization and segmentation of retinopathy (E). Table 1 lists references of the papers which addressed steps A–E either in part or in full. Full paper details are provided in the reference list.

Fig. 1 shows the number of papers which addressed each step in the processing sequence (A–E). Segmentation of the retinal vasculature (Step C) was a major area of focus within the literature, with 62 articles presenting techniques used for this step in the process. In contrast, less work was reported on localization of the macula and fovea (Step D).

Distribution of papers by image processing step A-E

Number of Articles
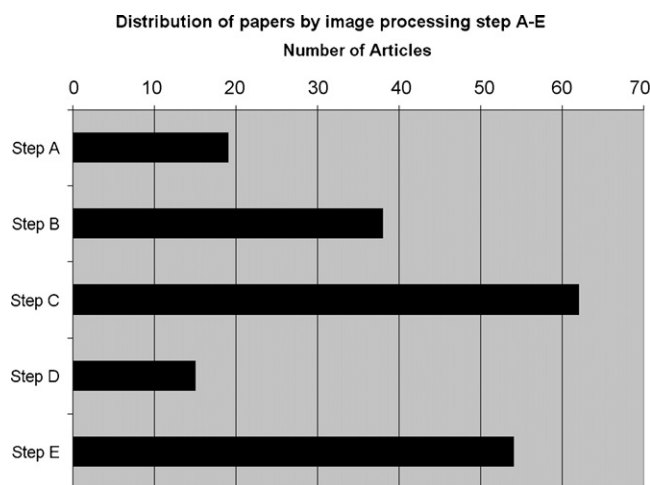
Fig. 1. Figure shows the categorization of literature by image processing step (pre-processing (Step A); localization and segmentation of the optic disk (Step B); segmentation of the retinal vasculature (Step C); localization of the macula and fovea (Step D); localization and segmentation of retinopathy (Step E)).

A total of 19 papers examined the preprocessing of images. Fig. 2 shows the range of approaches to preprocessing and the number of papers that addressed each method. Of the methods adopted, local contrast enhancement was the technology of choice in seven papers (36.8%), with other authors reporting on a variety of other techniques.

Localization of the optic disk and identification of the boundary was examined in 38 articles. Fig. 3 shows that localization was most frequently achieved by identifying the point of convergence of the main retinal blood vessels, or by using active contour models, snakes, principal components analysis (PCA) or the watershed transform. A number of articles combined PCA and snakes to achieve localization of the disk and definition of the boundary. However, methods such as simple identification of regions of high intensity pixels and adaptive thresholding along with others have also been developed.

Fig. 4 shows that two main techniques for vessel segmentation dominate this group. Of the reviewed articles, 27.4% used a vessel tracking technique, another 19.4% adopted matched filter techniques and the remainder focused on a variety of technologies,

including amongst others morphological analysis, PCA, wavelets and edge detection.

Determination of the position of the fovea and macula was covered by 15 articles, and was achieved almost exclusively by techniques that search for areas of lowest pixel intensity near the optic disk, usually within a radius of 2–2.5 disk diameters. This category had the lowest number of papers addressing the issue, indicating a lack of research in this area. However this may reflect the difficulty of automatically identifying these features, in isolation from other anatomical landmarks.
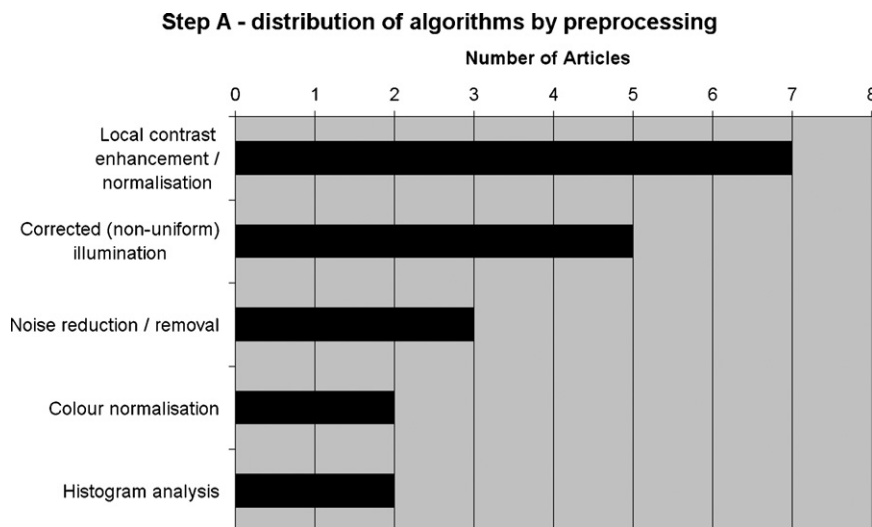
Fifty four articles focused on the detection of the pathological features of DR. These papers addressed methods for the detection of bright lesions such as hard exudates or cotton wool spots, and/or dark lesions such as microaneurysms and hemorrhages. However, it was not possible to categorize techniques used due to the wide range of pathological features to be identified. The types of techniques used included region growing, morphological analysis and classification algorithms.

Examining the reporting and evaluation methodologies, the following observations were made. Ninety percent of articles provided a reproducible description of their algorithms and evaluation methodology; sample sizes ranged between 1 and over 3700; 43% of papers used a defined standard against which to evaluate their algorithm(s); an objective outcome was reported in 75% of the papers; sensitivity and specificity were reported in 43% of articles.

4. Literature survey

A total of 127 papers were selected and analyzed. The algorithms described in these papers were classified in terms of five basic image processing and decision making categories and associated primary subdivisions as follows:

A. Preprocessing
   (1) Correction of non-uniform illumination.
   (2) Color normalization.
   (3) Contrast enhancement.
B. Localization and segmentation of the optic disk
   (1) Characteristics of the optic disk.
   (2) Optic disk localization.
   (3) Optic disk segmentation.
C. Segmentation of the retinal vasculature
   (1) Characteristics of the vasculature.
   (2) Methods for segmenting the vasculature.

Step A - distribution of algorithms by preprocessing

Number of Articles

Fig. 2. Figure shows the frequency of distribution of different preprocessing techniques.

Step B - localisation of optic disk

Number of Articles

Position of Vessels
Snakes / deformable models
Principal Components Analysis
Watershed Transform
Pixel intensity
Image (adaptive) thresholding
Pyramidal decomposition
Edge detection
Morphology
Hough transform
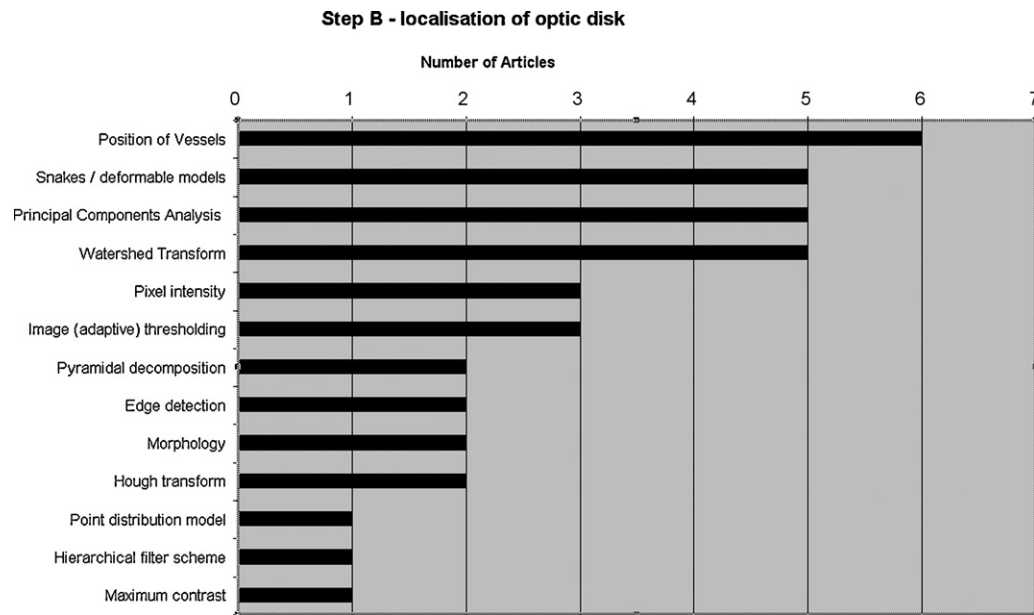Point distribution model
Hierarchical filter scheme
Maximum contrast

Fig. 3. Figure shows the frequency of distribution of approaches to optic disk localization.

D. localization of the macula and fovea
  (1) Characteristics of the macula and fovea.
  (2) Methods for localizing the macula and fovea.
E. Localization and segmentation of retinopathy
  (1) Microaneurysms/hemorrhages.
  (2) Exudates/cotton wool spots.

The following sections discuss each category in further detail. Where possible the relevant algorithms are described with suitable (additional) references, otherwise the reader is referred to the appropriate reference for an in-depth description.

4.1. Preprocessing of digital color retinal photographs (A)

The main objective of preprocessing techniques is to attenuate image variation by normalizing the original retinal image against a reference model or data set for subsequent viewing, processing or analysis. Variations typically arise within the same image (intra-image variability) as well as between images (inter-image variability) and in order to obtain meaningful information from an image, it is necessary to compensate for this variability. Intra-image variations arise due to differences in light diffusion, the presence of abnormalities, variation in fundus reflectivity and fundus thickness. Inter-image variability is particularly important for longitudinal studies. Differences between images may be caused by factors including differences in cameras, illumination, acquisition angle and retinal pigmentation.

The preprocessing of both monochromatic and color retinal images may be loosely classified in terms of the correction for non-uniform illumination, contrast enhancement and color normalization.

4.1.1. Correction of non-uniform illumination

Images are often described using an image formation model. A simple model describes a monochromatic image based upon illumination and reflectance components. Illumination is the amount of source light incident on a unit surface area. Reflectance is the ratio of the total amount of reflected light to the total illumination incident on a unit surface area. The illumination component of a digital retinal photograph is characterized by gradual non-uniform spatial variations, whilst the reflectance component tends to vary abruptly, particularly at the edges of anatomical features. According to Hoover and Goldbaum, this non-uniform illumination across the image results in shading artifacts and vignetting [3] hindering both quantitative image analysis and the reliable operation of subsequent global operators. The non-uniformities may not be visible to the human observer. However, they alter the local statistical characteristics of the image intensity including mean, median, and variance. This variability generally limits the reliability of subsequent methods for automated feature extraction and classification.

A number of general-purpose techniques have been investigated for attenuating this variation and improving the reliability of subsequent operators. Early approaches investigated space-variant filtering schemes supporting locally adaptive contrast enhancements [4]. High-pass filtering and mathematical modeling of the non-uniformity followed by subtraction of this component from the observed image [5] have also been investigated for the correction of non-uniform illumination. However, as noted by Foracchia et al. [6], general-purpose normalization operations typically use metrics derived from the whole image.

Several authors propose image formation models for describing the observed retinal images (e.g. Cree et al. [7]; Foracchia et al.
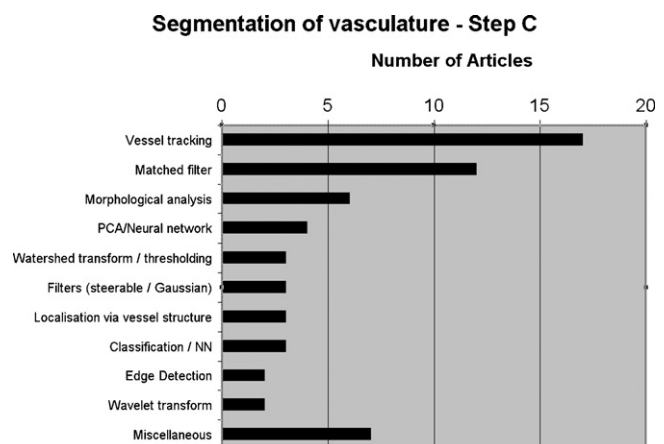
Segmentation of vasculature - Step C

Number of Articles

Vessel tracking
Matched filter
Morphological analysis
PCA/Neural network
Watershed transform / thresholding
Filters (steerable / Gaussian)
Localisation via vessel structure
Classification / NN
Edge Detection
Wavelet transform
Miscellaneous

Fig. 4. Figure shows the frequency of distribution of image processing techniques used to perform retinal vessel segmentation.

[8]), typically in terms of a foreground image, background image and an acquisition transformation function. The foreground image contains the vasculature, optic disk and any visible lesions. The background image contains all illumination variation due to the transformation function or the original background. This is the ideal image of the retina without any visible vascular structure or lesions. Several algorithms have been proposed based upon variations of this image formation model. Shade-correction is a method designed to remove non-uniform variations in the background image [9]. The background image is first approximated by smoothing the original image with a mean or median filter whose size is greater than the largest retinal feature. The original image may then be divided by the filtered image or the filtered image subtracted from the original. The literature reports the use of both procedures often without justification as to the use of one method over another [9–12]. Variations on the shade correction approach have also been proposed. Walter and Klein [13] apply alternating sequential filters to calculate the background approximation in order to avoid artifacts at the borders of bright regions. Wang et al. [14] proposed a method for correcting for non-uniform illumination based using a non-linear point transformation to correct image intensity. However, the principal limitation of approaches that estimate correction from the whole image is the inability to distinguish variations in luminance due to features from changes due to illumination.

This problem has been addressed by using the pixels associated with a specific retinal feature to contribute to the overall correction transformation. Wang et al. [15] proposes an approach based upon estimating gradual changes in illumination across vessel pixels, and its subtraction from the observed retinal image. However, there are several drawbacks to approaches which rely upon the detection of retinal anatomy. Firstly, the localization of retinal features such as specific vessels is a difficult task. Secondly, as noted by Foracchia et al. [6] the macular region has no discernible anatomy such as vessels from which to derive data in order to estimate illumination drift. Furthermore, there is significant variability in reflectance between arteries and veins. Foracchia et al. [6] propose an alternative approach based upon estimating the luminance and contrast variability in the background image. This parameterized model is then used to normalize the output image. This study is notable for the quantitative assessment of the effect of correcting for non-uniform illumination. The parametric model was compared to the method proposed by Wang et al. [14], a low-pass filter and a Wallis filter. The authors report a reduction in the variation in luminance and mean contrast in comparison to the other techniques.

4.1.2. Color normalization

Color is a powerful descriptor with significant potential as a means of discriminating between retinal features. Early work by Goldbaum et al. [16] identified differences in the color of different types of lesions in color retinal images. In part due to the hardware limitations, initial approaches for the automatic detection of retinal features operated primarily on the intensity component obtained either from "red-free" images or the green channel of RGB or fluorescein-labeled images. These monochrome components of the image tended to contain the most relevant diagnostic information. Furthermore, empirical observations by several authors (e.g. Shin et al. [17]; Leandro et al. [18]) identify the green channel of RGB images as containing the maximum contrast. Rapantzikos et al. [19] also note that the green channel appears to provide "more information" and is less subject to non-uniform illumination. The blue channel contains little useful information for the detection of retinal features. However, with improvements in the underlying imaging modalities, recently computed techniques have investigated the use of three color channels, as a means of distinguishing individual objects.

Color normalization is necessary due to the significant intra-image and inter-image variability in the color of the retina in different patients. Differences in skin pigmentation and iris color between different patients affect the coloration of the retina image. The age of the patient also affects retinal appearance and coloration. In adolescent patients specular reflection within the retina itself may result in artefactual features and coloration. Conversely, visual pigment and macular pigment density may be reduced with age (Berendschot et al. [20]). Ageing is also associated with lens coloration. Yellowing of the lens typically occurs in patients over 30. This increases the absorption of blue light leading to a variation in retinal appearance. The material composition of individual lesions will vary resulting in different reflection, absorption, and scattering properties. The color of the lesion can range from close to that of the background color to one with significant contrast. Non-uniform illumination across the image may also contribute to variations in color.

Recent work has investigated color normalization techniques for attenuating color variation. Sinthanayothin et al. [21] transformed the original retinal image to an intensity-hue-saturation representation. Hue is the dominant wavelength as perceived by a human observer. For example, a lesion of a certain type which appears as yellow or red is defined by its hue. Similarly, the relative "purity" of a color or the amount of achromatic light mixed with its hue is generally defined as the degree of saturation of a color. The separation of the different components allows the normalization of the intensity channel without changing the perceived relative color values of the pixels.

Histogram equalization redistributes the histogram of each color channel in the input image such that the output image contains a uniform pixel value distribution. The assumption is that for each color plane the pixel rank order is maintained even with variations in illumination. A monotonic, non-linear transformation function is applied to equalize the histogram of each separate color channel. An output image is produced by applying the function to map each grey level value in the input image to a new corresponding value in the output image. Peaks and valleys will remain after equalization but the distribution may be shifted or "spread" out. However, a limitation of relying upon equalization is that it is only possible to produce a single approximation to a uniform histogram. This may not always provide the desired effect. The histogram equalization of retinal images tends to over-emphasize the contribution of the blue channel information since the normal retina usually reflects little blue light [22]. Furthermore, equalization may be ineffective in attenuating inter-image variation in retinal images intended for longitudinal analysis.

Histogram specification is an alternative form of histogram processing for color normalization. The distribution of each color channel is interpolated to more closely match that of a reference model. The reference model is usually obtained from an image judged by an expert to have good contrast and coloration to maximize the performance of an automated detection technique. Histogram specification is typically comprised of two stages. First, the histogram of each color channel of the original image is equalized. Second, an inverse transformation function is applied to determine (an approximation of) the desired histogram for each color channel in the output image.

In a recent study, Goatman et al. [23] compared histogram specification and equalization algorithms for color normalization. The effect of normalization was determined by plotting the chromaticity values of cotton wool spots, drusen, blot hemorrhages and hard exudates after each method of color normalization. Inspection of the resulting chromaticity graphs indicated that histogram specification achieved the greatest separation between lesion type clusters after color normalization. However, a quantitative assessment of the compared normalization algorithms was not reported.

Osareh et al. [24] applied histogram specification to ensure that all the sample images matched a reference image distribution. However, a limitation of matching a retinal image to a reference model is the potential for masking specific lesion characteristics within the resultant histogram. Redistributing the histogram to match that of a reference image, which does not necessarily contain the lesion, may obscure evidence of the pathology. For example, exudates have a yellow white appearance which results in a peak in the histogram of the green channel. This may be removed if histogram specification to a retinal image not containing exudates is used. Recent work by Cree et al. [25] addresses this problem using both shade correction and histogram normalization. This proposed algorithm retained the overall shape of the histogram and transformed the hue to be consistent between images.

4.1.3. Contrast enhancement

In "vision science", contrast defines the perceived brightness or color variation within an image. Contrast enhancement techniques are aimed at altering the visual appearance that makes an object (or its representation in an image) distinguishable from other objects and the background. The contrast of relatively simple images containing uniform regions on a uniform background and the contrast of colored text on a uniform background is usually measured using a weighted ratio of the difference in the perceived luminance of an object and its immediate surroundings.

The use of a luminance ratio may be appropriate when measuring attributes of grayscale sinusoids or uniform patches. However, as noted by Calabria and Fairchild [26] the use of maximum and minimum luminance pixels may not correspond with the perceived contrast within a complex image. There are no widely accepted metrics for the measurement of color contrast enhancement. The performance of various enhancement techniques is typically quantified either by subjective visual inspection of the output image or by measuring improvement in the machine recognition task as a result of enhancement.

The literature describes a number of methods for contrast enhancement in order to more readily discern retinal features. These preprocessing steps are usually applied to retinal images after correcting for non-uniform illumination and color normalization. Retinal images acquired using standard clinical protocols often exhibit low contrast and may contain photographic artifacts. Several authors (for example, Usher et al. [27]; Osareh [22]) also note that retinal images typically have a higher contrast in the centre of the image with reduced contrast moving outward from the centre. Conventional methods based upon global histogram techniques for normalizing or enhancing image contrast such as contrast stretching and histogram equalization tend to result in information loss in both the brighter and darker areas of a retinal image. Contrast manipulation within retinal images is usually addressed using a two-stage approach comprised of local contrast enhancement (LCE) and noise reduction respectively. LCE methods enhance small regions of interest although any noise within the image is also amplified resulting in artifactual features. This effect is visible particularly in areas with few features such as the central region of the macula. The LCE methods are based upon the use of small windows as local transforms after correcting for non-uniform illumination. Sinthanayothin et al. [21] propose an adaptive contrast enhancement transformation dependent upon the mean and variance of the intensity within a local region. The transformation operation is applied to the intensity component of an HSI representation of the image which has been smoothed to attenuate background noise. This adaptive transformation provides a large increase in contrast in regions with an initially small variance (poor contrast) and little contrast enhancement for an initially large variance (high contrast).

Similar adaptive LCE methods have also been investigated for the enhancement of specific features. These methods typically follow a hierarchical approach intended to manipulate the local histogram distributions within a specified region. Rapantzikos et al. [19] propose a multilevel histogram equalization (MLE) method as a preprocessing step in the detection of drusen. The approach is based on the sequential application of histogram equalization to progressively smaller non-overlapping neighborhoods. The size of the neighborhood is always larger than the target lesion. However, the detection of multiple types of anatomy and pathology with different physical dimensions is also problematic when relying upon a hierarchal neighborhood method. The dimensions of the neighborhoods are highly dependent on the size of the lesion within the image. The neighborhood may be small enough to fit within a lesion resulting in the introduction of artifactual contrast variations.

4.2. Localization and segmentation of the optic disk (B)

The literature generally defines the localization of the optic disk as the identification of the centre of the disk either by specifying the centre of the optic disk or placing a mask within a particular region of the retina. Segmentation of the optic disk usually refers to the subsequent task of determining the contour of the disk. Localization and segmentation of the optic disk are important tasks in retinal image analysis. The disk centre and contour are often prerequisite landmarks in establishing a frame of reference for identifying retinal anatomy and pathology. The dimensions of the disk may be used to calibrate measurements in retinal images; for example, the fovea, which is the centre of vision, is located between the major temporal retinal vessels approximately 2.5 disk diameters temporal to the temporal edge of the optic disk [28]. Localizing the optic disk is also a prerequisite for the computation of some important diagnostic indices for hypertensive/sclerotic retinopathy based on vasculature, such as central retinal artery equivalent and central retinal vein equivalent (Hubbard et al. [29]). Finally, the retinal vessels emanate from the centre of the optic disk. Therefore, the disk may be used as a starting point for vessel tracking methods (Lalonde et al. [30]).

4.2.1. Visual characteristics of the optic disk

The optic disk is the visible part of the optic nerve head within the retina. The optic disk is approximately elliptical in shape with a vertical meridian (width 1.8 ± 0.2 mm, height 1.9 ± 0.2 mm) [21]. The absence of the pigmented epithelium renders the color of the optic disk paler than the surrounding retina. Such areas of disk paleness, or pallor, tend to be yellowish or white in color. Nerve fibers reach the optic nerve head, turn and pass through the optic nerve, causing a small central depression called the physiologic cup. Major branches of the central retinal artery emanate from the disk, and bifurcate to form branch vessels diverging from the main vessel. Venous vessels converge at the disk into the central retinal vein. These vessels may obscure parts of the disk rim. The contour of the optic disk is usually defined as the inner margin of the peripapillary scleral ring. The contour of the rim typically has variable contrast, with the nasal side usually less bright than the temporal side. The area of pallor may appear as a smaller, brighter disk within the optic disk. There may also be bright regions near the edge of the disk caused by peripapillary atrophy.

There is significant normal variation in the appearance of the optic disk. The size and shape of the physiologic cup varies amongst individuals. The optic disk is generally brighter than the surrounding area with a clearly discernible elliptical contour. However, it may also appear as a hollow ring. In any case the cup appears as a smaller, brighter region within the optic disk. The nasal side of the optic nerve head is typically less bright than the temporal side and occasionally not visible at all. Variation in pigmentation within

normal eyes also causes differences in the appearance of the disk. Another unique aspect of each optic nerve head is the pattern of the retinal vasculature crossing the disk contour.

4.2.2. Optic disk localization

Localizing the centre and rim of the disk is often necessary to differentiate the disk from other features of the retina and as an important landmark. Techniques described in the literature for optic disk localization are typically aimed at either identifying the approximate centre of the optic disk or placing the disk within a specific region such as a circle or square. In either case, localization is complicated by the presence of strong "distractors". Distractors include vessel edges, spatially varying albedo, peripapillary atrophy and large exudative lesions. These features typically have similar attributes to the optic disk such as intensity, color and contrast. Early work generally assumed that the grey level variation in the papillary region was higher than in any other part of the image (e.g. Chaudhuri et al. [31]). The optic disk was localized by identifying the largest cluster of bright pixels. Algorithms which rely solely on intensity variation proved simple, fast and reasonably robust for optic disk localization in normal retinal images with negligible variation between images. However, an optic disk obscured by blood vessels or only partially visible may be misidentified using methods based solely upon identifying the brightest regions. Such methods are also highly sensitive to distractors such as yellow/white lesions or bright artifactual features [32].

Characteristics of the optic disk including intensity, morphology and color have been investigated for localizing the disk in the presence of distractors. Sinthanayothin et al. [21] used an 80×80 pixel sub-image to evaluate the intensity variance of adjacent pixels. The point with the largest variance was assumed to be the centre of the optic disk. The assumption is that visible signs of disease such as exudates will have a lower intensity variance than the optic disk. The authors report a 99.1% sensitivity and specificity in localizing the centre of the optic disk in images with little or no visible signs of lesions. However, Lowell et al. [28] report the misidentification of the optic disk using this algorithm in retinal images with a large number of white lesions, light artifacts or strongly visible choroidal vessels. Osareh [22] proposes a similar technique using a 110×110 pixel template image obtained by averaging the optic disk region in 25 retinal images. He reports successfully localizing the approximate centre of the optic disk in 75 out of 75 images.

The Hough transform has been investigated by a number of authors for the localization of the optic disk (e.g. Yulong and Dingru [33]; Pinz et al. [34]; Liu et al. [35]; Kochner et al. [36]; Ege et al. [37]; Lowell et al. [28]; Chrastek et al. [38]). The underlying principle used to identify the optic disk is to consider that a retinal image is comprised of an infinite number of potential circles which pass through a number of edge points. The edge points are derived from edge information extracted by applying one of several available edge detection algorithms. The Hough transform determines which of these potential circles intersect with the greatest number of circles in the image. Each data point in effect votes for an infinite number of parameter sets and the parameter set with the highest total vote is taken as the solution. Liu et al. [35] used a circular Hough transform after edge detection to localize the optic disk in the red color channel. The first stage searched for an optic disk candidate region defined as a 180×180 pixel region that included the brightest 2% of grey level values. A Sobel operator was applied to detect the edge points of the candidate region and the contours were then detected by means of the circular Hough transform. Kochner et al. [36] proposed a combination of a Hough transform and steerable filters to automatically detect the location and size of the disk. Points belonging to the edges of the main vessel branches are extracted using first-order Gaussian filter kernels at varying orientations. The edges of the vessels are fitted to an ellipse via a Hough transform

and the location of the optic disk is approximated from one end of the ellipse major axis. The Hough transform is highly tolerant of gaps in feature contour descriptions and is relatively unaffected by image noise. This is useful when attempting to isolate the optic disk which often does not have a clearly defined edge and is broken by vessels. However, Hough spaces tend to be sensitive to the spatial resolution of the image [3]. In addition, the prerequisite edge detection algorithms often fail to provide an acceptable solution due to the fuzzy boundaries, inconsistent image contrast or missing edge features in the disk region.

Principal components analysis has also been used as a means of extracting common features of retinal images including the optic disk and blood vessels (Li and Chutatape [39]; Sanchez et al. [40]; Sinthanayothin et al. [21]). The PCA procedure projects the original correlated features described in a vector format onto a new, smaller uncorrelated space, called principal components. The first principal component lies along the axis that shows the highest variance in the data. The covariance matrix of the data is computed, and Eigenvalues of the matrix are ordered in a decreasing manner. Several authors have used PCA to extract common features from retinal images (Li and Chutatape [39]; Sanchez et al. [40]). The likelihood of a candidate region being an optic disk was determined by comparing the characteristics of the optic disk extracted from a training image to those derived from an unseen image. Li and Chutatape [39] report the correct localization of the optic disk in 99% of 89 images.

Lalonde et al. [41] propose a pyramidal decomposition technique in combination with Hausdorff-based template matching. First, potential regions containing the optic disk were located by means of a pyramidal decomposition of the green channel image using the Harr discrete wavelet transform. The lowest resolution level has a small image size, thus reducing the visibility of small bright regions associated with lesions such as exudates. Pixels in the lowest resolution image which have the highest intensity values compared with the mean pixel intensity were denoted as candidate regions. Next, the optic disk was localized using the Hausdorff distance to compare the candidate region to a circular template with dimensions approximating the optic disk. The Hausdorff distance provides a measure of the degree of mismatch between two sets of points where a Hausdorff distance of zero indicates an ideal match. A notable aspect of the described approach is the reliance upon a priori knowledge of the image characteristics. Image descriptors include whether the image is of a left or right eye and whether the input image is centered on the macula or optic disk. This reduces the search area and assigns a confidence value to each candidate region. Lalonde et al. [41] report the correct localization (without identifying the contour) of the optic disk in 40 of 40 images with a mean overlap of 80%. In each case the disk was indicated by positioning a circular template over the candidate region. However, as noted by Lowell et al. [28] the use of pyramidal decomposition and template-matching may prove overly complex, with similar results achievable using less complex algorithms.

Alternative techniques have been investigated which use different features of the retina such as blood vessels as a means of localizing the optic disk. Akita and Kuga [42] proposed a vessel tracking technique to trace the parent–child relationship between blood vessel segments towards a point of convergence assumed to be the centre of the optic disk. The approach is based upon identifying the strongest vessel network convergence as the primary feature for detection using blood vessel binary segmentation. The intensity of the optic disk was also used as a secondary feature to localize the disk. Hoover et al. [3,43] also propose the convergence of blood vessels as a means of localizing the centre of the optic disk. The approach correctly identified the optic disk location in 89% of 81 images, 50 of which were diseased retinas. Another recent approach proposed by Foracchia et al. [8] localizes the optic disk by fitting a parametric geometrical model of the retinal vascular

system to the main vessels extracted from the image. The vascular structure is first segmented to provide accurate measurements of the vessel center point position, diameter and direction. The geometrical model of the retina is then fitted to the main vessels within the image to localize the center of the optic disk. The model is also parameterized according to the different rates of vascular curvature in the nasal and temporal regions. The parameters are optimized with respect to the vessel directions measured at points belonging to the vascular structure. The use of the vasculature means that it is possible to approximate the location of an optic disk which is not visible within the image. As noted by Foracchia et al. [8], the estimated position of the optic disk may be compared with the location intuitively reconstructed from anatomical knowledge. However, as previously discussed, the prerequisite step of segmenting the vascular network is itself a complex and difficult task. Techniques for extraction of the vasculature are affected by bright lesions and artifactual features such as specular reflectance or visible choroidal vessels (Lowell et al. [28]). For example, false positive responses in the detection of individual vessels may be caused by the edges of bright lesions and the edge of the optic disk contour (Hoover et al. [44]). This misclassification of the vasculature may degrade the performance of subsequent methods aimed at identifying the other parts of the retina such as the optic disk. The impact of incorrectly identifying the vasculature on subsequent algorithms for localizing the optic disk is unclear. Foracchia et al. [8] investigated the use of a geometrical model of the vasculature structure as a means of detecting the optic disk. The optic disk was correctly localized in 79 of 81 images using the two algorithmically different methods for vasculature segmentation namely, binary segmentation (Hoover et al. [44]) and sparse-tracking (Foracchia et al. [45]). Each method resulted in misclassification of the optic disk in different images. However, the overall performance in relation to the detection of the optic disk was unchanged.

4.2.3. Optic disk segmentation

Optic disk contour segmentation is usually performed after identifying the approximate centre of the disk. Identifying the contour of the optic disk is a non-trivial problem. The natural variation in the characteristics of the optic disk including the previously described differences in pigmentation and myelination of the nerve fiber layer are significant problems for defining the contour of the disk. Blood vessels may cross the boundary of the optic disk obscuring the rim of the disk with the edges of vessels also acting as significant distractors.

The literature describes a number of algorithms for determining the disk contour. Walter and Klein [46] describe an approach using color space transformation and morphological filtering techniques for disk localization. The optic disk was first localized using the luminance channel of the hue-luminance-saturation (HLS) color space and a thresholding operation was applied to determine the approximate locus of the optic disk. The precise contour of the disk was then determined, using the red channel of the RGB color space, via a "watershed transform". In determining the optic disk, the transform is constrained by markers derived from the previously calculated approximation of disk center to prevent over-segmentation of the disk region. Walter and Klein [46] report correctly localizing the optic disk in 29 out of 30 retinal images. The contour of the optic disk was identified in 27 of the 29 often with slight distortion of the contour due to outgoing vessels or low contrast.

Algorithms for optic disk segmentation based upon *active contours or snakes* have been investigated by several authors. Kass et al. [47] proposed the concept of a deformable contour that changes its shape depending on properties of the image, desired contour properties or knowledge based constraints. The behavior of classical parametric active contours is controlled by internal and external energy functions (or forces). The minimization of the total energy function moves the contour towards the target shape. The external energies direct the snake towards certain features, such as edges, in the image. The internal energies such as elasticity and rigidity serve as a smoothness constraint to resist the deformation. The contour itself is typically represented by a vector of control points the movement of which adjust the snakes. When a minimum is reached the contours are smooth and reside on object boundaries. Early work by Lee and Brady [48] exploited an active contour to determine the boundary of the optic disk. However, a quantitative assessment of the approach was not presented in the paper. Mendels et al. [49,50] investigated applying a morphological operator followed by an active contour to segment the disk. A dilation operator was first applied, followed by an erosion operator to re-establish the optic disk contour. Finally, a morphological reconstruction operator was applied by maintaining the maximum of the dilated/eroded image and the original one. Having removed the blood vessels crossing the disk boundary, an active contour was initialized as a circle centered on and inside the optic disk. The contour was fitted to the rim of the disk using the gradient vector flow (GVF) technique (Xu and Prince [51]). The technique was tested against a set of nine retinal images. The authors reported an accurate segmentation of the optic disk contour in all nine images. However, as noted by Lowell et al. [28], the published images appear to be of relatively high quality and it is likely the performance of the algorithm would be significantly degraded when applied to a greater number of test images exhibiting a significant variation in the quality and content.

More recent work by Osareh [22] has proposed two key extensions in the use of GVF snakes for optic disk segmentation. The optic disk was first localized using the previously described template matching or regression arc algorithm. Secondly, color morphological processing was used to obtain a more homogeneous inner disk area, which increased the accuracy of the snake initialization. An overall accuracy of 91.84% was reported in comparison to the reference standard of a clinical ophthalmologist. Lowell et al. [28] proposed a similar two-stage approach. The optic disk was first localized using a template matching technique. A specialized three phase elliptical global and local deformable model with variable edge-strength dependent stiffness was then fitted to the contour of the disk. The algorithm was evaluated against a randomly selected database of 100 images from a diabetic screening programme. Ten images were classified as unusable; the others were of variable quality. The algorithm successfully identified the optic disk contour in 89 of 90 randomly chosen low-resolution diabetic retinal images using a contour-model-based approach, based upon a technique developed by Hu et al. [52] for vessel cross-sectional boundary extraction in magnetic resonance image studies.

4.3. Segmentation of the retinal vasculature (C)

The segmentation and measurement of the retinal vessels is of primary interest in the diagnosis and treatment of a number of systemic and ophthalmologic conditions. As previously discussed, the accurate segmentation of the retinal blood vessels is often an essential prerequisite step in the identification of retinal anatomy and pathology. In addition, the segmentation of the vessels is useful for image registration or spatial alignment of images. The registration of images, which are often acquired using different modalities, is a critical operation in parametric imaging and the longitudinal monitoring of retinal appearance.

4.3.1. Characteristics of the retinal vasculature

The retinal vasculature is composed of the arteries and veins, with their tributaries, which are visible within the retinal image. The central retinal artery bifurcates at or on the optic disk into divisions that supply the four quadrants of the inner retinal layers. A

similarly arranged system of retinal veins joins at the optic disk. The vessels have a lower reflectance compared to other retinal surfaces, thus, they appear darker relative to the background. Light is absorbed and reflected by the retinal vessels, the retinal capillaries and the choroid. Variations in the thickness of the vessel wall and the index of refraction have negligible influence on the apparent width of the blood column. However, occasionally a light streak running the length of the vessel is reflected from the transparent convex wall of the arteriole (Lowell et al. [53]). Light reflexes and artifactual features such as specular reflection are typically found in the retinal images of younger patients. However, the thickening and fibrosis of the vessel wall associated with arteriosclerosis changes the refractive index and increases the width of the light reflex.

4.3.2. Matched filtering

Matched filtering for the detection of the vasculature convolves a 2D kernel with the retinal image. The kernel is designed to model some feature in the image at some unknown position and orientation, and the matched filter response (MFR) indicates the presence of the feature. Three primary characteristics determine properties of the kernel. Vessels usually have a limited curvature and may be approximated by piecewise linear segments; the diameter of the vessels decreases as they move radially outward from the optic disk; and the cross-sectional pixel intensity profile of these line segments approximates a Gaussian curve.

Chaudhuri et al. [54] proposed a two-dimensional linear kernel with a Gaussian profile for segmentation of the vasculature. The profile of the filter is designed to match that of a blood vessel, which typically has a Gaussian or a Gaussian derivative profile. The kernel is typically rotated in 30–45° increments to fit into vessels of different orientations. The highest response filter is selected for each pixel and is typically thresholded to provide a vessel image. Further post processing is then applied to identify vessel segments. As noted by several authors (Patton et al. [55]; Heneghan et al. [56]) a MFR method is effective when used in conjunction with additional processing techniques. However, the convolution kernel may be quite large and needs to be applied at several rotations resulting in a computational overhead which may reduce the performance of the overall segmentation approach. In addition, the kernel responds optimally to vessels that have the same standard deviation of the underlying Gaussian function specified by the kernel. As a consequence, the kernel may not respond to vessels that have a different profile. The retinal background variation and low contrast of the smaller vessels also increase the number of false responses around bright objects such as exudates and reflection artifacts. Other objects within the image such as the boundaries of the optic nerve and some hemorrhages and lesions, can exhibit the same local attributes as vessels. There are also problems associated with detecting very fine neovascularization partly due to image resolution. In addition, the use of an overly long structuring element may cause difficulty in fitting into highly tortuous vessels. Several authors have proposed refinements and extensions which address many of these problems (Chaudhuri et al. [54]; Kochner et al. [36]; Hoover et al. [44]; Lowell et al. [53]; Yang et al. [57]).

4.3.3. Morphological processing and curvature estimation

The basic morphology of the vasculature is known a priori to be comprised of connected linear segments. Morphological operators have been applied to vasculature segmentation (Zana and Klein [58,59]) and also to microaneurysm extraction. Morphological processing for identifying specific shapes has the advantage of speed and noise resistance. Gregson et al. [60] utilize morphological closing to help identify veins in the automated grading of venous beading by filling in any "holes" in the silhouette of the vein created during the processing procedure. The main disadvantage of exclusively relying upon morphological methods is that they do not exploit the known vessel cross-sectional shape.

4.3.4. Vessel tracking

Vessel tracking algorithms segment a vessel between two points. Unlike the previously described techniques for vasculature segmentation they work at the level of a single vessel rather than the entire vasculature. A vessel tracking approach typically steps along the vessel. The centre of the longitudinal cross-section of vessel is determined with various properties of the vessel including average width and tortuosity measured during tracking. The main advantage of vessel tracking methods is that they provide highly accurate vessel widths, and can provide information about individual vessels that is usually unavailable using other methods. Unfortunately, they require the starting point, and usually the end point, of a vessel to be defined by a user and are thus, without additional techniques, of limited use in fully automated analysis. In addition, vessel-tracking techniques may be confused by vessel crossings and bifurcations (Frame et al. [61]). Teng et al. [62] address several of these problems by proposing the use of matched filters.

4.3.5. Pixel-based classification

Several authors have investigated a number of classification methods for the segmentation of the vessels. Artificial neural networks have been extensively investigated for segmenting retinal features such as the vasculature (Akita and Kuga [42]) making classifications based on statistical probabilities rather than objective reasoning. These neural networks employ mathematical "weights" to decide the probability of input data belonging to a particular output. This weighting system can be adjusted by training the network with data of known output typically with a feedback mechanism allowing retraining.

Sinthanayothin et al. [21] preprocessed images with PCA to reduce background noise by reducing the dimensionality of the data set and then applied a neural network to identify the pathology. They reported a success rate of 99.56% for training data and 96.88% for validation data, respectively, with an overall sensitivity and specificity of 83.3% (standard deviation 16.8%) and 91% (standard deviation 5.2%), respectively. The result of the approach was compared with an experienced ophthalmologist manually mapping out the location of the blood vessels in a random sample of seventy-three 20×20 pixel windows and requiring an exact match between pixels in both images.

A significant disadvantage of neural networks is the necessity for configuring the network with training data or a 'gold standard'. This gold standard data set consists of a number of images whose vascular structure must be precisely marked by an ophthalmologist. However, as noted by Hoover et al. [44] there is significant disagreement in the identification of vessels even amongst expert observers.

4.4. Localization of the fovea and macula (D)

Temporal to the optic nerve head is the macula which appears darker in color and has no blood vessels present in the centre. The fovea lies at the centre of the macula and is the part of the retina that is used for fine vision. Retinopathy in this area, termed maculopathy, is associated with a high risk of visual loss. The macula is a dark approximately circular area, but the contrast is often quite low and it may be obscured somewhat by exudates or hemorrhages. As a consequence a search to obtain a global correlation often fails. The fovea is located approximately 2–2.5 disk diameters temporal to the temporal edge of the optic disk and between the major temporal retinal vascular arcades (e.g. Li et al. [63]; Narasimha-Iyer et al. [64]). These positional constraints can be used to identify a small search area for the macula, and to estimate the position if the

search fails, although variation in the optic disk size compromises the reliability of this method. The detection of the macula and fovea is mainly determined by estimating the position in relation to other retinal features (e.g. Tobin et al. [65]).

4.5. Detection of diabetic retinopathy (E)

4.5.1. Clinical features of diabetic retinopathy

Diabetic retinopathy is one of the commonest microvascular complications of diabetes. It signifies damage to the microvasculature of the retina and although the pathogenic mechanisms are not fully understood, the clinical features are typical and easily recognized. Microaneurysms, small outpouchings of the capillary walls, are the first microvasular changes to appear and are sentinel markers for early diabetic retinopathy. With disease progression small intra-retinal dot hemorrhages, often indistinguishable from microaneurysms appear, and later larger blot hemorrhages. Excessive capillary permeability is manifest as retinal edema usually accompanied by lipid exudation. If at the macula this can be seriously sight threatening (diabetic maculopathy). Increasing capillary dysfunction leads to inner retinal ischemia with the development of micro infarcts (cotton wool spots), intra-retinal microvascular abnormalities (IRMA) and later abnormal new vessel formation (proliferative diabetic retinopathy).

4.5.2. Detection of microaneurysms/hemorrhages

As with other algorithms designed for the segmentation of retinal anatomy, early work in the automated detection of pathology generally investigated fluorescein angiography and "red-free" images. Initial techniques relied upon global image-processing procedures. Several authors investigated the segmentation of microaneurysms from the background retinal image by grey level thresholding after segmenting anatomy. Binary morphological processing and structuring elements in the thresholded images allows further discrimination between microaneurysms and other features, such as small vessel sections.

Spencer et al. [9] proposed a morphological transformation to segment microaneurysms within fluorescein angiograms. The shade-corrected image was first "opened" by applying an erosion operator, followed by dilation. An 11-pixel linear kernel was then applied in eight rotational orientations that, when combined, included all of the vessel sections and excluded all the circular microaneurysms. This opened image was extracted from the original shade-corrected image using a "top-hat transformation" producing an image that only contained microaneurysms. The authors reported a sensitivity of 82% and specificity of 86% in comparison to a clinician, with 100 false positive pixels per image reported. However, only four images were included and the method of comparing the computed output to that of the clinician was not described.

Cree et al. [66] refined this technique using alternative region-growing and classification algorithms. This approach automatically determined the macular region and included an automated process for image registration to allow sequential comparisons of microaneurysm turnover, based on a registration of longitudinal images. However, the authors reported that the automated registration process for sequential studies often failed for poor-quality images and those with prior laser photocoagulation. The reason for failure in either case was not described. Automated selection of the macular region of interest was reported as being accurate in 93 of 95 images. The images were obtained from individual patients with varying degrees of retinopathy. The images contained 297 microaneurysms defined by the joint agreement of an ophthalmologist and a medical physicist. The automated detection algorithm achieved a sensitivity of 82%, and specificity of 84% in previously unseen image data.

Goatman et al. [67] proposed a technique for the detection and longitudinal monitoring of microaneurysms in fluorescein angiography. Using the approach developed by Cree et al. [66], the turnover of microaneurysms (static, new or regressed) was compared with a reference standard of an ophthalmologist experienced in identifying microaneurysms and grading of retinopathy in angiographic images. Compared with manual measurements of nine manual graders, the automated system was fast and reliable with similar sensitivity and specificity to manual graders.

Hipwell et al. [68] proposed a method for the detection of microaneurysms in red-free images. The images were initially processed by shade correction of the image, followed by removal of vessels and other distractors by the top-hat transformation. A Gaussian matched filter was applied to retain candidate microaneurysms for subsequent classification. The classification algorithm was based on 13 different parameters derived from a training set of 102 images of variable degrees of retinopathy. The parameters included shape, intensity, circularity, perimeter length and length ratio. The study used a total of 3783 images from 589 patients on 977 visits. The images were graded for "presence/absence of microaneurysms" and/or "hemorrhages" against the reference standard of an experienced clinical research fellow according to the EURODIAB HMA protocol (Aldington et al. [69]). The system produced a sensitivity of 81%, with 93% specificity. However, this was only achieved when images with questionable HMA present were excluded.

A number of authors have investigated neural networks for the detection of pathology. An early approach by Gardner et al. [70] used a back propagation neural network to detect microaneurysms and/or hemorrhages. Initial training was performed on 147 diabetic and 32 normal images, analyzing the green channel from 601 color images, and dividing images into 20×20 pixel or 30×30 pixel windows, which were each individually graded manually by a trained observer. The sub-images were classified as "normal without vessel", "normal vessel", "exudate" and "hemorrhage/microaneurysm". This information was used as the training set prior to using a previously unseen testing set. The authors reported detection rates for hemorrhages of 73.8% for both sensitivity and specificity, compared with the reference standard of a clinical ophthalmologist, based upon 200 diabetic and 101 normal images. When classifying images into "normal", "diabetic requiring referral" and "diabetic not requiring referral", based on the reference standard of the clinical ophthalmologist, they reported a sensitivity of 88.4% and a specificity of 83.5%. Increasing the sensitivity to 99% resulted in a fall in the specificity to 69%.

Sinthanayothin et al. [71] used the previously described recursive region-growing technique and adaptive intensity thresholding in conjunction with a "moat operator". The operator increases the contrast of the lesions by enhancing the edges. A recursive region-growing segmentation algorithm was applied to the image and a neural network was then used to extract the retinal blood vessels. For a total of 30 images (14 of which contained hemorrhages/microaneurysms), they reported a sensitivity and specificity for hemorrhage/microaneurysm detection as 77.5% and 88.7%, respectively (clinical ophthalmologist as the reference standard). Again the method of comparison was not described in detail.

Usher et al. [27] also employed a neural network, based on 451 macula-centred color images. After preprocessing and segmentation of anatomy, hemorrhages/microaneurysms were extracted using recursive region growing and adaptive intensity thresholding in conjunction with a "moat operator" (Sinthanayothin et al. [71]). Training was performed on 500 patients before analysis of performance in comparison with a trained clinical diabetologist (audited by a consultant ophthalmologist) in 773 patients. On a per patient basis, sensitivity for detection of any exudates and/or hemorrhages/microaneurysms was 95.1% (95% confidence interval (CI) 92.3–97.7%) and specificity was 46.3% (95% CI 41.6–51%). For detec-

tion of diabetic retinopathy, maximum sensitivity and specificity were 70.8% and 78.9%, respectively.

A number of authors reported the outcome of algorithms for the automatic detection of pathology (Lee et al. [72]; Larsen et al. [73]). The result of the processing is described in a clinical context, however, no details regarding the nature of the processing or pattern recognition were provided. Lee et al. [72] employed color fundus photographs and image processing (image enhancement, noise removal and image normalization) in conjunction with pattern recognition to test for particular features of yearly diabetic retinopathy. A sensitivity of 77% and specificity of 94% is reported when compared with a general ophthalmologist.

4.5.3. Detection of retinal exudates and cotton wool spots

Sinthanayothin et al. [71] identified exudates in color images based on the same recursive region-growing technique described above to define an "exudate" and "non-exudate" image. After thresholding to produce a binary image, the regions containing the exudates were overlaid onto the original image. The authors reported a sensitivity and specificity (with reference to a clinical ophthalmologist grading images manually) of 88.5% and 99.7%, respectively, for 30 images (21 of which contained exudates). Gardner et al. [70] reported a sensitivity of 93.1% using the previously described approach based upon neural networks.

Ege et al. [37] reported the detection of exudates and cotton wool spots with sensitivity of 99% and 80%, respectively. In comparison with a general clinical ophthalmologist, Lee et al. [72] reported sensitivities of 96% and 80% and specificities of 93% and 93% for hard exudates and cotton wool spots.

5. Discussion

A structured survey of algorithms for the automatic detection of retinopathy in digital color retinal images has been presented. The development of an effective tool for incorporation into diabetic retinopathy screening programmes is a highly desirable goal. An efficient system that can routinely analyze digital retinal images and eliminate those where no new or increased pathology is present, would significantly reduce the workload for ophthalmologists and graders in diabetic retinopathy screening centres. This review has focused completely on the analysis of digital color images of the retina in the field of diabetic retinopathy.

The process of analyzing a digital color image of the retina may be viewed as a series of steps, for each of which, a choice of technologies or algorithms is available. Firstly, the performance of an algorithm for the detection of anatomy and pathology can be visually and quantitatively assessed in terms of the overall performance of the system. Secondly the individual steps within the algorithm may also be individually assessed. The efficiency of each step must be high, to ensure that the effectiveness of the overall process is maintained at a satisfactory level of sensitivity and specificity. Although significant advances have been made in the application of digital imaging technology to this field, it remains a challenge to identify the optimal series of algorithms that would comprise a successful automated image screening system for DR. In this survey, the diversity of the identified studies made it impossible to conduct a full quantitative statistical analysis of the performance of each processing step within the various approaches. Our descriptive statistics show which techniques have been used most frequently in each of the steps. Whilst frequency of use does not necessarily indicate best practice, it does give an indication of which techniques have been most thoroughly evaluated. The qualitative analysis allowed articles to be grouped according to the methodological approaches used for each step in the process, and trends within the literature to be identified. It is recognized that in most cases, the existing methodologies have some shortcomings, and

many of the articles set out to develop improved methodologies derived from an existing technique. It is very hard for researchers to determine which are the best algorithms to employ at each step to ensure the most efficient throughput of images. This is supported by Abramoff et al. [74] where they conclude that "automated detection of diabetic retinopathy using published algorithms cannot yet be recommended for clinical practice".

A key issue in the automated detection of anatomy and pathology is the difficulty in identifying the gold-standard or ground-truth. As observed by numerous studies there are significant differences in regions of interest identified by expert observers. The clinical significance of discrepancies between observers is also highly specific to the image. A questionable lesion in a critical region such as the fovea has greater clinical significance than that at another location. Further research studies are required that evaluate each step of the analysis process and report the sensitivity and specificity of each step and the process as a whole.

A wide range of study population/sample size was observed across the literature reviewed, sample sizes ranged from a single image to over 3700 individual images. It is recognized that a variety of methods are required for different types of research and that a large sample size is not always necessary. Perhaps, clear guidelines in image processing research would be helpful to avoid producing results/data that are difficult to compare in terms of the success of the algorithms or techniques.

It was observed that there was a trend towards increasing sample size with studies published more recently compared to earlier studies. This may be due to increased availability of digital data in recent years and a move towards evaluation rather than development of methodologies. Abramoff et al. [74] suggest that performance of algorithms should be evaluated on publicly available validated digital image libraries. The availability of web based digital image libraries such as STARE provide open-access digital image data. Originally developed in 1975, STARE provides 397 ophthalmological images with a variety of diagnoses http://www.parl.clemson.edu/stare/). The DRIVE database (http://www.isi.uu.nl/Research /Databases/DRIVE/) has been established to facilitate comparative studies on segmentation of blood vessels in retinal images. The research community is invited by them to test their algorithms on this database and share the results with other researchers through the web site.

In addition, digital image processing research into DR could benefit from the creation of a large training set of images that could be accessed by investigators for evaluation of their systems. Current data sharing initiatives endorsed by research councils and other funders should facilitate the creation of such a database. Finally, the authors recommend that the development of successful screening systems for diabetic retinopathy would be greatly facilitated by the adoption of a standard format for reporting of such studies such as that recommended by Bossuyt et al. [75], who presented the STARD statement for the reporting of studies analyzing the performance of diagnostic tests.

References

[1] Wild S, Roglic G, Green A, Sicree R, King H. Global prevalence of diabetes: estimates for the year 2000 and projections for 2030. Diabetes Care 2004;27:1047–53.

[2] Sharp PF, Olson J, Strachan F, Hipwell J, Ludbrook A, O'Donnell MT, et al. The value of digital imaging in diabetic retinopathy. Health Technol Assess 2003;7:1–119.

[3] Hoover A, Goldbaum M. Locating the optic nerve in a retinal image using the fuzzy convergence of the blood vessels. IEEE Trans Med Imaging 2003;22:951–8.

[4] Wallis R. An approach to the space variant restoration and enhancement of images. In: Proceedings of the symposium on current mathematical problems in imaging science. 1976. p. 329–40.

[5] Gonzalez, Woods. Digital Image Processing. Prentice Hall; 2002.

[6] Foracchia M, Grisan E, Ruggeri A. Luminosity and contrast normalization in retinal images. Med Imaging Anal 2005;9:179–90.

[7] Cree MJ, Olson JA, McHardy KC, Sharp PF, Forrester JV. The preprocessing of retinal images for the detection of fluorescein leakage. Phys Med Biol 1999;44:293–308.

[8] Foracchia M, Grisan E, Ruggeri A. Detection of optic disc in retinal images by means of a geometrical model of vessel structure. IEEE Trans Med Imaging 2004;23:1189–95.

[9] Spencer T, Olson JA, McHardy KC, Sharp PF, Forrester JV. An image-processing strategy for the segmentation and quantification of microaneurysms in fluorescein angiograms of the ocular fundus. Comp Biomed Res 1996;29:284–302.

[10] Jagoe R, Arnold J, Blauth C, Smith PLC, Taylor KM, Wootton K. Measurement of capillary dropout in retinal angiograms by computerised image analysis. Pattern Recogn Lett 1992;13:143–51.

[11] Ward NP, Tomlinson S, Taylor CJ. Image analysis of fundus photographs: the detection and measurement of exudates associated with diabetic retinopathy. Ophthalmology 1989;96:80–6.

[12] Øien G, Osnes P. Diabetic retinopathy: automatic detection of early symptoms from retinal images. In proceedings of NORSIG-95 Norwegian signal processing symposium 1995. Available at http://www.ux.his.no/sigproc/www/norsig/norsig95.html.

[13] Walter T, Klein J-C. A computational approach to diagnosis of diabetic retinopathy. In: Proceedings of the 6th conference on systemics, cybernetics and informatics (SCI). 2002. p. 521–6.

[14] Wang H, Hsu W, Goh KG, Lee ML. An effective approach to detect lesions in color retinal images. In: IEEE conference on computer vision and pattern recognition. 2000. p. 1–6.

[15] Wang Y, Tan W, Lee SC. Illumination normalization of retinal images using sampling and interpolation. Proc SPIE Med Imaging 2001: Image Process 2001;4322:500–7.

[16] Goldbaum MH, Katz NP, Nelson MR, Haff LR. The discrimination of similarly colored objects in images of the ocular fundus. Invest Ophthalmol Vis Sci 1990;31:617–23.

[17] Shin DS, Javornik NB, Berger JW. Computer-assisted, interactive fundus image processing for macular drusen quantitation. Ophthalmology 1999;106:1119–25.

[18] Leandro JJG, Soares JVB, Cesar Jr RM, Jelinek HF. Blood vessels segmentation in nonmydriatic images using wavelets and statistical classifiers. In: XVI Brazilian symposium on computer graphics and image processing. 2003. p. 262–9.

[19] Rapantzikos K, Zervakis M, Balas K. Detection and segmentation of drusen deposits on human retina: potential in the diagnosis of age-related macular degeneration. Med Imaging Anal 2003;7:95–108.

[20] Berendschot TT, DeLint PJ, van Norren D. Fundus reflectance-historical and present ideas. Prog Retin Eye Res 2003;22:171–200.

[21] Sinthanayothin C, Boyce JF, Cook HL, Williamson TH. Automated localisation of the optic disc, fovea, and retinal blood vessels from digital color fundus images. Br J Ophthalmol 1999;83:902–10.

[22] Osareh A. Automated identification of diabetic retinal exudates and the optic disc. Ph.D. thesis. University of Bristol; 2004.

[23] Goatman KA, Whitwam AD, Manivannan A, Olson JA, Sharp PF. Color normalisation of retinal images. In: Proceedings medical image understanding and analysis. 2003. p. 49–52.

[24] Osareh A, Mirmehdi M, Thomas B, Markham R. Automated identification of diabetic retinal exudates in digital color images. Br J Ophthalmol 2003;87:1220–3.

[25] Cree MJ, Gamble E, Cornforth D. Color normalisation to reduce inter-patient and intra-patient variability in microaneurysm detection in color retinal images, WDIC2005 ARPS workshop on digital image computing, Brisbane, Australia, 2005. p. 163–8.

[26] Calabria AJ, Fairchild MD. Perceived image contrast and observer preference I. the effects of lightness, chroma, and sharpness manipulations on contrast perception. J Imaging Sci Technol 2003;47:479–93.

[27] Usher D, Dumskyj M, Himaga M, Williamson TH, Nussey S, Boyce J. Automated detection of diabetic retinopathy in digital retinal images: a tool for diabetic retinopathy screening. Diabet Med 2004;21:84–90.

[28] Lowell J, Hunter A, Steel D, Basu A, Ryder R, Fletcher E, et al. Optic nerve head segmentation. IEEE Trans Med Imaging 2004;23:256–64.

[29] Hubbard LD, Brothers RJ, King WN, Clegg LX, Klein R, Cooper LS, et al. Methods for evaluation of retinal microvascular abnormalities associated with hypertension/sclerosis in the atherosclerosis risk in communities study. Ophthalmology 1999;106:2269–80.

[30] Lalonde M, Gagnon L, Boucher M-C. Non-recursive paired tracking for vessel extraction from retinal images. In: Proceedings of the conference vision interface. 2000. p. 61–8.

[31] Chaudhuri S, Chatterjee S, Katz N, Nelson M, Goldbaum M. Automatic detection of the optic nerve in retinal images. In: IEEE international conference on imaging processing, vol. 1. 1989. p. 1–5.

[32] Goldbaum M, Moezzi S, Taylor A, Chatterjee S, Boyd J, Hunter E, et al. Automated diagnosis and image understanding with object extraction, object classification, and inferencing in retinal images. In: Proceedings IEEE international conference on image processing, vol. 3. 1996. p. 695–8.

[33] Yulong M, Dingru X. Recognizing the glaucoma from ocular fundus image by image analysts. In: Proceedings of the 12th international conference of the IEEE engineering in medicine and biology society. 1990. p. 178–9.

[34] Pinz A, Bernogger S, Datlinger P, Kruger A. Mapping the human retina. IEEE Trans Med Imaging 1998;17:606–19.

[35] Liu Z, Chutatape O, Krishnan SM. Automatic image analysis of fundus photograph. In: Proceedings 19th international conference IEEE engineering in medicine and biology society. 1997. p. 524–5.

[36] Kochner B, Schuhmann D, Michaelis M, Mann G, Englmeier K-H. Course tracking and contour extraction of retinal vessels from color fundus photographs: most efficient use of steerable filters for model based image analysis. In: SPIE conference image processing, vol. 3338. 1998. p. 755–61.

[37] Ege BM, Hejlesen OK, Larsen OV, Moller K, Jennings B, Kerr D, et al. Screening for diabetic retinopathy using computer based image analysis and statistical classification. Comput Methods Programs Biomed 2000;62:165–75.

[38] Chrastek R, Wolf M, Donath K, Niemann H, Paulus D, Hothorn T, et al. Automated segmentation of the optic nerve head for diagnosis of glaucoma. Med Image Anal 2005;9:297–314.

[39] Li H, Chutatape O. Automated feature extraction in color retinal images by a model based approach. IEEE Trans Biomed Eng 2004;51:246–54.

[40] Sanchez CI, Hornero R, Lopez MI, Poza J. Retinal image analysis to detect and quantify lesions associated with diabetic retinopathy. In: Proceedings of the 26th annual international conference of the IEEE engineering in medicine and biology society, vol. 1. 2004. p. 1624–7.

[41] Lalonde M, Beaulieu M, Gagnon L. Fast and robust optic disc detection using pyramidal decomposition and Hausdorff-based template matching. IEEE Trans Med Imaging 2001;20:1193–200.

[42] Akita K, Kuga H. A computer method of understanding ocular fundus images. Pattern Recognit 1982;15:431–43.

[43] Hoover A, Goldbaum M. Fuzzy convergence. In: Proceedings IEEE computer society conference on computer vision and pattern recognition. 1998. p. 716–21.

[44] Hoover A, Kouznetsova V, Goldbaum M. Locating blood vessels in retinal images by piecewise threshold probing of a matched filter response. IEEE Trans Med Imaging 2000;19:203–10.

[45] Foracchia M, Grisan E, Ruggeri A. Detection of vessel caliber irregularities in color retinal fundus images by means of fine tracking. In: Proceedings of the 2nd European medical and biological engineering conference. 2002.

[46] Walter T, Klein J-C. Segmentation of color fundus images of the human retina: detection of the optic disc and the vascular tree using morphological techniques. In: Second international symposium on medical data analysis. 2001. p. 282–7.

[47] Kass M, Witkin A, Terzopoulos D. Snakes: active contour models. Int J Comput Vis 1987;1:321–31.

[48] Lee S, Brady M. Integrating stereo and photometric stereo to monitor the development of glaucoma. Image Vision Comput 1991;9:39–44.

[49] Mendels F, Heneghan C, Harper PD, Reilly RB, Thiran J-Ph. Extraction of the optic disk boundary in digital fundus images. In: Proceedings of the first joint BMES/EMBS conference. 1999. p. 1139.

[50] Mendels F, Heneghan C, Thiran J–Ph. Identification of the optic disc boundary in retinal images using active contours. In: In the proceedings of the Irish machine vision and image processing conference. 1999. p. 103–15.

[51] Xu C, Prince JL. Snakes, shapes, and gradient vector flow. IEEE Trans Image Process 1998;7:359–69.

[52] Hu YL, Rogers WJ, Coast DA, Kramer CM, Reichek N. Vessel boundary extraction based on a global and local deformable physical model with variable stiffness. Mag Reson Imaging 1998;16:943–51.

[53] Lowell J, Hunter A, Steel D, Basu A, Ryder R, Kennedy RL. Measurement of retinal vessel widths from fundus images based on 2-D Modeling. IEEE Trans Med Imaging 2004;23:1196–204.

[54] Chaudhuri S, Chatterjee S, Katz N, Nelson M, Goldbaum M. Detection of blood vessels in retinal images using two-dimensional matched filters. IEEE Trans Med Imaging 1989;8:263–9.

[55] Patton N, Aslam TM, Macgillivray T, Deary IJ, Dhillon B, Eikelboom RH, et al. Retinal image analysis: concepts, applications and potential. Prog Retin Eye Res 2006;25:99–127.

[56] Heneghan C, Flynn J, O'Keefe M, Cahill M. Characterization of changes in blood vessel width and tortuosity in retinopathy of prematurity using image analysis. Med Image Anal 2002;6:407–29.

[57] Yang C-W, Ma D-J, Chao S-C, Wang C-M, Wen CH, Lo SC, et al. A computer-aided diagnostic detection system of venous beading in retinal images. Opt Eng 2000;39:1293–303.

[58] Zana F, Klein JC. Robust segmentation of vessels from retinal angiography. In: Proceedings of international conference on digital signal processing. 1997. p. 1087–90.

[59] Zana F, Klein J. A multimodal registration algorithm of eye fundus images using vessels detection and Hough transform. IEEE Trans Med Imaging 1999;18:419–28.

[60] Gregson P, Shen Z, Scott R, Kozousek V. Automated grading of venous beading. Comput Biomed Res 1995;28:291–304.

[61] Frame AJ, Undrill PE, Cree MJ, Olson JA, McHardy KC, Sharp PF, et al. A comparison of computer based classification methods applied to the detection of microaneurysms in ophthalmic fluorescein angiograms. Comput Biol Med 1998;28:225–38.

[62] Teng T, Lefley M, Claremont D. Progress towards automated diabetic ocular screening: a review of image analysis and intelligent systems for diabetic retinopathy. IEEE Med Biol Eng Comput 2002;40:2–13.

[63] Li H, Chutatape O. A model-based approach for automated feature extraction in fundus image. In: Proceedings of the ninth IEEE international conference on computer vision, vol. 1. 2003. p. 394–9.

[64] Narasimha-Iyer H, Can A, Roysam B, Tanenbaum HL, Majerovics A. Integrated analysis of vascular and nonvascular changes from color retinal fundus image sequences. Biomed Eng IEEE Trans 2007;54(8):1436–45.

[65] Tobin KW, Chaum E, Govindasamy VP, Karnowski TP. Detection of anatomic structures in human retinal imagery. IEEE Trans Med Imag 2007;26(12):1729–39.

[66] Cree MJ, Olson JA, McHardy KC, Sharp PF, Forrester JV. A fully automated comparative microaneurysm digital detection system. Eye 1997;11:622–8.

[67] Goatman KA, Cree MJ, Olson JA, Sharp PF, Forrester JV. Automated measurement of microaneurysm turnover. Invest Ophthalmol Vis Sci 2003;44:5335–41.

[68] Hipwell JH, Strachan F, Olson JA, McHardy KC, Sharp PF, Forrester JV. Automated detection of microaneurysms in digital red-free photographs: a diabetic retinopathy screening tool. Diab Med 2000;17:588–94.

[69] Aldington SJ, Kohner EM, Meuer S, Klein R, Sjolie AK. Methodology for retinal photography and assessment of diabetic retinopathy: the EURODIAB IDDM complications study. Diabetologia 1995;38:437–44.

[70] Gardner G, Keating D, Williamson TH, Ell AT. Automatic detection of diabetic retinopathy using an artificial neural network: a screening tool. Br J Ophthalmol 1996;80:940–4.

[71] Sinthanayothin C, Boyce JF, Williamson TH, Cook HL, Mensah E, Lal S, et al. Automated detection of diabetic retinopathy on digital fundus images. Diabet Med 2002;19:105–12.

[72] Lee SC, Lee ET, Kingsley RM, Wang Y, Russell D, Klein R, et al. Comparison of diagnosis of early retinal lesions of diabetic retinopathy between a computer system and human experts. Arch Ophthalmol 2001;119:509–15.

[73] Larsen N, Godt J, Grunkin M, Lund-Andersen H, Larsen M. Automated detection of diabetic retinopathy in a fundus photographic screening population. Invest Ophthalmol Vis Sci 2003;44:767–71.

[74] Abràmoff MD, Niemeijer M, Suttorp-Schulten MS, Viergever MA, Russell SR, van Ginneken B. Evaluation of a system for automatic detection of diabetic retinopathy from color fundus photographs in a large population of patients with diabetes. Diabetes Care 2008;31(2):193–8.

[75] Bossuyt PM, Reitsma JB, Bruns DE, Gatsonis PP, Glasziou PP, Irwig LM, et al. Standards for reporting of diagnostic accuracy. toward complete and accurate reporting of studies of diagnostic accuracy: the STARD initiative. Standards for Reporting of Diagnostic Accuracy. Clin Chem 2003;49:19–20.

[76] Abdel-Razik Y, Ghalwash AZ, Abdel-Rahman Ghoneim AAS. Optic disc detection from normalized digital fundus images by means of a vessels' direction matched filter. IEEE Trans Med Imaging 2008;27(1):11–8.

[77] Abdurrazaq I, Hati S, Eswaran C. Morphology approach for features extraction in retinal images for diabetic retionopathy diagnosis. Comput Commun Eng 2008:1373–7.

[78] Badea P, Danciu D, Davidescu L. Preliminary results on using an extension of gradient method for detection of red lesions on eye fundus photographs. Automation, quality and testing, robotics, IEEE international conference 2008;3:43–8.

[79] Can A, Shen H, Turner JN, Tanenbaum HL, Roysam B. Rapid automated tracing and feature extraction from retinal fundus images using direct exploratory algorithms. IEEE Trans Inf Technol Biomed 1999;3:125–38.

[80] Can A, Stewart CV, Roysam B, Tanenbaum HL. A feature-based, robust, hierarchical algorithm for registering pairs of images of the curved human retina. IEEE Trans Pattern Anal Mach Intell 2002;24:347–64.

[81] Can A, Stewart CV, Roysam B, Tanenbaum HL. A feature-based technique for joint, linear estimation of high-order image-to-mosaic transformations: mosaicing the curved human retina. IEEE Trans Pattern Anal Mach Intell 2002;24:412–9.

[82] Chanwimaluang T, Fan G. An efficient blood vessel detection algorithm for retinal images using local entropy thresholding. In: Proceedings of the international symposium on circuits and systems, vol. 5. 2003. p. 21–4.

[83] Chanwimaluang T, Fan GL, Fransen SR. Hybrid retinal image registration. IEEE Trans Inform Technol Biomed 2006;10:129–42.

[84] Chapman N, Witt N, Gao X, Bharath AA, Stanton AV, Thom SA, et al. Computer algorithms for the automated measurement of retinal arteriolar diameters. Br J Ophthalmol 2001;85:74–9.

[85] Chutatape O, Zheng L, Krishnan S. Retinal blood vessel detection and tracking by matched Gaussian and Kalman filters. In: Proceedings of IEEE EMBS, vol. 20. 1998. p. 3144–9.

[86] Chutatape O, Li H. Ocular fundus coordinate establishment. In: proceedings of the 24th engineering in medicine and biology annual conference and the annual fall meeting of the biomedical engineering society conference, vol. 3. 2002. p. 2141–2.

[87] Cornforth DJ, Jelinek HJ, Leandro JJG, Soares JVB, Cesar Jr RM, Cree MJ, et al. Development of retinal blood vessel segmentation methodology using wavelet transforms assessment of diabetic retinopathy. In: Eighth Asia pacific symposium on intelligent and evolutionary systems. 2004. p. 50–60.

[88] David J, Krishnan Rekha A, Sukesh K. Neural network based retinal image analysis. Congress Image Signal Process 2008;2:49–53.

[89] Dua S, Kandiraju N, Thompson HW. Design and implementation of a unique blood-vessel detection algorithm towards early diagnosis of diabetic retinopathy. In: International conference on information technology: coding and computing, vol. 1. 2005. p. 26–31.

[90] Estabridis K, de Figueiredo RJP. Automatic detection and diagnosis of diabetic retinopathy. In: IEEE international conference on image processing, vol. 2. 2007. p. 445–8.

[91] Estabridis K, de Figueiredo R. Blood vessel detection via a multi-window parameter transform. In: 19th IEEE international symposium on computer-based medical systems. 2006. p. 424–9.

[92] Eswaran C, Reza AW, Hati S. Extraction of the contours of optic disc and exudates based on marker-controlled watershed segmentation. In: International conference on computer science and information technology. 2008. p. 719–23.

[93] Fang B, Hsu W, Lee ML. Reconstruction of vascular structures in retinal images. In: Proceedings international conference on image processing, vol. 2. 2003. p. 157–60.

[94] Fleming AD, Goatman KA, Philip S, Olson JA, Sharp PF. Automatic detection of retinal anatomy to assist diabetic retinopathy screening. Phys Med Biol 2007;52(2):331–45.

[95] Fleming AD, Philip S, Goatman KA, Williams GJ, Olson JA, Sharp PF. Automated detection of exudates for diabetic retinopathy screening. Phys Med Biol 2007;52(24):7385–96.

[96] Gagnon L, Lalonde M, Beaulieu M, Boucher M-C. Procedure to detect anatomical structures in optical fundus images. Proc SPIE Med Imaging: Image Process 2001;4322:1218–25.

[97] Gang L, Chutatape O, Krishnan SM. Detection and measurement of retinal vessels in fundus images using amplitude modified second-order Gaussian filter. IEEE Trans Biomed Eng 2002;49:168–72.

[98] Gang L, Chutatape O, Lui H, Krishnan SM. Abnormality detection in automated mass screening system of diabetic retinopathy. In: Proceedings of 14th IEEE symposium on computer-based medical systems. 2001. p. 132–7.

[99] Gao XW, Bharath A, Stanton A, Hughes A, Chapman N, Thom S. Quantification and characterisation of arteries in retinal images. Comput Methods Programs Biomed 2000;63:133–46.

[100] Gao XW, Bharath A, Stanton A, Hughes A, Chapman N, Thom S. Measurement of vessel diameters on retinal images for cardiovascular studies. In: Proceedings medical image understanding and analysis. 2001.

[101] Gao X, Bharath A, Stanton A, Hughes A, Chapman N, Thom S. A method of vessel tracking for vessel diameter measurement on retinal images. In: Proceedings international conference on image processing, vol. 2. 2001. p. 881–4.

[102] Garcia M, Hornero R, Sanchez CI, Lopez MI, Diez A. Feature extraction and selection for the automatic detection of hard exudates in retinal images. In: 29th annual international conference of the IEEE engineering in medicine and biology society. 2007. p. 4969–72.

[103] Goh KG, Hsu W, Lee ML, Wang H. ADRIS: an automatic diabetic retinal image screening system. In: Cois KJ, editor. Medical data mining and knowledge discovery, 60, studies in fuzziness and soft computing. Physica-Verlag; 2001. p. 181–210.

[104] Grisan E, Pesce A, Giani A, Foracchia M, Ruggeri A. A new tracking system for the robust extraction of retinal vessel structure. In: Proceedings of IEEE international conference engineering and biology society. 2004. p. 1620–3.

[105] Grisan E, Ruggeri A. Segmentation of candidate dark lesions in fundus images based on local thresholding and pixel density. In: 29th international conference of the IEEE engineering in medicine and biology society. 2007. p. 6735–8.

[106] Hajer J, Kamel H, Noureddine E. Localization of the optic disk in retinal image using the 'watersnake'. In: International conference on computer and communication engineering. 2008. p. 947–51.

[107] Hansen AB, Hartvig NV, Jensen MS, Borch-Johnsen K, Lund-Andersen H, Larsen M. Diabetic retinopathy screening using digital non-mydriatic fundus photography and automated image analysis. Acta Ophthalmol Scand 2004;82:666–72.

[108] Hayashi J-I, Takamitsu K, Cole J, Soga R, Hatanaka Y, Lu M, et al. A development of computer-aided diagnosis system using fundus images. In: Seventh international conference on virtual systems and multimedia. 2001. p. 429.

[109] Hong S, Roysam B, Stewart CV, Turner JN, Tanenbaum HL. Optimal scheduling of tracing computations for real-time vascular landmark extraction from retinal fundus images. IEEE Trans Inform Technol Biomed 2001;5:77–91.

[110] Hong S, Stewart CV, Roysam B, Gang L, Tanenbaum HL. Frame-rate spatial referencing based on invariant indexing and alignment with application to online retinal image registration. IEEE Trans Pattern Anal Mach Intell 2003;25:379–84.

[111] Hsu W, Pallawala PMDS, Mong LL, Kah-Guan AE. The role of domain knowledge in the detection of retinal hard exudates. In: Proceedings IEEE computer society conference on computer vision and pattern recognition, vol. 2. 2001. p. 246–51.

[112] Hwee KL, Chutatape O. Blood vessel tracking technique for optic nerve localisation for field 1–3 color fundus images. In: Proceedings of the joint conference of the fourth international conference on information, communications and signal processing, and the fourth pacific rim conference on multimedia, vol. 3. 2003. p. 1437–41.

[113] Iqbal MI, Aibinu AM, Nilsson M, Tijani IB, Salami MJE. Detection of vascular intersection in retina fundus image using modified cross point number and neural network technique. Int Conf Comput Commun Eng 2008:241–6.

[114] Jiang X, Mojon D. Adaptive local thresholding by verification-based multi-threshold probing with application to vessel detection in retinal images. IEEE Trans Pattern Anal Mach Intell 2003;25:131–7.

[115] Kahai P, Namuduri KR, Thompson H. Decision support for automated screening of diabetic retinopathy. In: Conference record of the thirty-eighth asilomar conference on signals, systems and computers, vol. 2. 2004. p. 1630–2344.

[116] Kahai P, Namuduri KR, Thompson H. A decision support framework for automated screening of diabetic retinopathy. Int J Biomed Imaging 2006:1–8.

[117] Lalonde ML, Gagnon M-C. Boucher automatic visual quality assessment in optical fundus images. In: Proceedings of vision interface. 2001. p. 259–64.

[118] Lee SS, Rajeswari M, Ramachandram D, Shaharuddin B. Screening of diabetic retinopathy—automatic segmentation of optic disc in colour fundus images. In: The second international conference on distributed frameworks for multimedia applications. 2006. p. 1–7.

[119] Lee S, Wang Y, Tan W. Automated detection of venous beading in retinal images. Proc SPIE Med Imaging Process 2001;4322:1365–72.

[120] Li H, Chutatape O. Fundus image features extraction. In: Proceeding of 22nd IEEE international conference engineering in medicine and biology society. 2000. p. 3071–3.

[121] Li H, Chutatape O. Automatic location of the optic disk in retinal images. In: Proceedings of IEEE international conference imaging processing. 2001. p. 837–40.

[122] Li H, Hsu W, Lee ML, Wong TY. Automatic grading of retinal vessel caliber. IEEE Trans Biomed Eng 2005;52:1352–5.

[123] Luo G, Chutatape O, Li H, Krishnan SM. Abnormality detection in automated mass screening system of diabetic retinopathy. In: Proceedings 14th IEEE symposium on computer-based medical systems. 2001. p. 132–7.

[124] Mahadevan V, Narasimha-Iyer H, Roysam B, Tanenbaum HL. Robust model-based vasculature detection in noisy biomedical images. IEEE Trans Inform Technol Biomed 2004;8:360–76.

[125] Martínez-Pérez ME, Hughes AD, Stanton AV, Thom SA, Chapman N, Bharath AA, et al. Retinal vascular tree morphology: a semi-automatic quantification. IEEE Trans Biomed Eng 2002;49:912–7.

[126] Narasimha-Iyer H, Can A, Roysam B, Stewart CV, Tanenbaum HL, Majerovics A, et al. Robust detection and classification of longitudinal changes in color retinal fundus images for monitoring diabetic retinopathy. IEEE Trans Biomed Eng 2006;53(6):1084–98.

[127] Nayak J, Bhat PS, Acharya UR, Lim CM, Kagathi M. Automated identification of diabetic retinopathy stages using digital fundus images. J Med Syst 2008;32(2):107–15.

[128] Niemeijer M, van Ginneken B, Staal J, Suttorp-Schulten MSA, Abramoff MD. Automatic detection of red lesions in digital color fundus photographs. IEEE Trans Med Imaging 2005;24:584–92.

[129] Niemeijer M, Van Ginneken B, Russell SR, Suttorp-Schulten MSA, Abramoff MD. Automated detection and differentiation of drusen, exudates, and cotton–wool spots in digital color fundus photographs for diabetic retinopathy diagnosis. Invest Ophthalmol Vis Sci 2007;48(5):2260–7.

[130] Niemeijer M, Abramoff MD, van Ginneken B. Segmentation of the optic disc, macula and vascular arch in fundus photographs. IEEE Trans Med Imaging 2007;26(1):116–27.

[131] Niemeijer M, Staal JJ, van Ginneken B, Loog M, Abràmoff MD. Comparative study of retinal vessel segmentation methods on a new publicly available database. In: Fitzpatrick JM, Sonka M, editors. SPIE medical imaging, vol. 5370. 2004. p. 648–56.

[132] Noronha K, Nayak J, Bhat SN. Enhancement of retinal fundus image to highlight the features for detection of abnormal eyes. In: TENCON 2006. IEEE region 10 conference. 2006. p. 1–4.

[133] Osareh A, Mirmehdi M, Thomas B, Markham R. Comparison of color spaces for optic disc localisation in retinal images. In: Proceedings of 16th international conference on pattern recognition, vol. 1. 2002. p. 743–6.

[134] Pallawala PMDS, Hsu W, Lee ML, Goh SS. Automated microaneurysm segmentation and detection using generalized Eigenvectors. In: Seventh IEEE workshop on application of computer vision, vol. 1. 2005. p. 322–7.

[135] Pedersen L, Grunkin M, Ersbøll B, Madsen K, Larsen M, Christoffersen N, et al. Quantitative measurement of changes in retinal vessel diameter in ocular fundus images. Pattern Recogn Lett 2000;21:1215–23.

[136] Pham TD, Tran DT, Brown M, Kennedy RL. Image segmentation of retinal vessels by fuzzy models. In: Proceedings of 2005 international symposium on intelligent signal processing and communication systems. 2005. p. 541–4.

[137] Quellec G, Lamard M, Josselin PM, Cazuguel G, Cochener B, Roux C. Detection of lesions in retina photographs based on the wavelet transform. In: 28th annual international conference of the IEEE engineering in medicine and biology society. 2006. p. 2618–21.

[138] Quellec G, Lamard M, Josselin PM, Cazuguel G, Cochener B, Roux C. Optimal wavelet transform for the detection of microaneurysms in retina photographs. IEEE Trans Med Imaging 2008;27(9):1230–41.

[139] Raman B, Bursell ES, Wilson M, Zamora G, Nemeth SC, Soliz P. The effects of spatial resolution on an automated diabetic retinopathy screening system's performance in detecting microaneurysms for diabetic retinopathy. In: Proceedings of the 17th IEEE symposium on computer-based medical systems, CBMS. 2004. p. 128–33.

[140] Sagar AV, Balasubramaniam S, Chandrasekaran V. A novel integrated approach using dynamic thresholding and edge detection (IDTED) for automatic detection of exudates in digital fundus retinal images. In: International conference on computing: theory and applications. 2007. p. 705–10.

[141] Sanchez Clara I, Mayo A, GarciaM, LopezMI, Hornero R. Automatic image processing algorithm to detect hard exudates based on mixture models. In: 28th annual international conference of the IEEE engineering in medicine and biology society. 2006. p. 4453–6.

[142] Saradhi GV, Balasubramanian S, Chandrasekaran V. Performance enhancement of optic disc boundary detection using active contours via improved homogenization of optic disc region. In: International conference on information and automation. 2006. p. 264–9.

[143] Satyarthi D, Raju BAN, Dandapat S. Detection of diabetic retinopathy in fundus images using vector quantization technique. In: Annual India conference. 2006. p. 1–4.

[144] Sekhar S, Al-Nuaimy W, Nandi AK. Automated localisation of retinal optic disk using Hough transform. In: 5th IEEE international symposium on biomedical imaging: from nano to macro. 2008. p. 1577–80.

[145] Sinthanayothin C, Kongbunkiat V, Phoojaruenchanachai S, Singalavanija A. Automated screening system for diabetic retinopathy. In: Proceedings of the 3rd international symposium on image and signal processing and analysis, ISPA, vol. 2. 2003. p. 915–20.

[146] Simandjuntak RA, Suksmono AB, Mengko TLR, Sovani I. Development of computer-aided diagnosis system for early diabetic retinopathy based on micro aneurysms detection from retinal images. In: Proceedings of 7th international workshop on enterprise networking and computing in healthcare industry, 2005. HEALTHCOM. 2005. p. 364–7.

[147] Staal JJ, Abramoff MD, Niemeijer M, Viergever MA, van Ginneken B. Ridge based vessel segmentation in color images of the retina. IEEE Trans Med Imaging 2004;23:501–9.

[148] Tan W, Wang Y, Lee S. Retinal blood vessel detection using frequency analysis and local-mean-interpolation filters. In: Proceedings of SPIE Vol Med Imaging: Image Processing, vol. 4322. 2001. p. 1373–84.

[149] Truitt P, Soliz P, Farnath D, Nemeth S. Utility of color information for segmentation of digital retinal images: neural network-based approach. SPIE Med Imaging: Image Process 1998;3338:1470–81.

[150] Tsai C-L, Stewart CV, Tanenbaum HL, Roysam B. Model-based method for improving the accuracy and repeatability of estimating vascular bifurcations and crossovers from retinal fundus images. IEEE Trans Inform Technol Biomed 2004;8:122–30.

[151] Vallabha D, Dorairaj R, Namuduri K, Thompson H. Automated detection and classification of vascular abnormalities in diabetic retinopathy. In: Conference record of the thirty-eighth asilomar conference on signals, systems and computers, vol. 2. 2004. p. 1625–9.

[152] Walter T, Klein J-C. Automatic detection of microaneurysms in color fundus images of the human retina by means of the bounding box closing. In: Third international symposium on medical data analysis. 2002. p. 210–20.

[153] Walter T, Klein J-C, Massin P, Erginay A. A contribution of image processing to the diagnosis of diabetic retinopathy—detection of exudates in color fundus images of the human retina. IEEE Trans Med Imaging 2002;21:1236–43.

[154] Walter T, Massin P, Erginay A, Ordonez R, Jeulin C, Klein J-C. Automatic detection of microaneurysms in color fundus images. Med Image Anal 2007;11(6):555–66.

[155] Xiaohui Z, Chutatape O. A SVM approach for detection of hemorrhages in background diabetic retinopathy. In: IEEE international joint conference on neural networks, vol. 4. 2005. p. 2435–40.

[156] Xiaohui Z, Chutatape O. Top-down and bottom-up strategies in lesion detection of background diabetic retinopathy. In: IEEE computer society conference on computer vision and pattern recognition, vol. 2. 2005. p. 422–8.

[157] Yang G, Wang S, Gagnon L, Boucher M-C. Algorithm for detecting microaneurysms in low-resolution color retinal images. In Proc Vision Interface 2001:265–71.

[158] Zhang X, Chutatape O. Detection and classification of bright lesions in color fundus images. In: International conference on image processing, vol. 1. 2004. p. 139–42.

John R. Winder graduated from the University of Ulster in physics and chemistry in 1983. He attained an MSc in physics in 1985 from University College of Wales and a PhD in 2004 from University of Ulster. He worked as medical physicist for 15 years and is now a reader in Medical Imaging at the University of Ulster. His research interests include medical image visualisation, 3D modeling and rapid prototyping.

Philip J. Morrow is currently a senior lecturer in the School of Computing and Information Engineering in the Faculty of Computing and Engineering at the University of Ulster, Northern Ireland. He has a BSc in applied mathematics and computer science (1981), an MSc in electronics (1982) and a PhD in parallel image processing (1993), all from the Queen's University of Belfast. His main research interests lie in image processing, machine vision and parallel/distributed computing.

Ian N. McRitchie received his BSc and PhD degrees in Computer Science form the Queen's University Belfast in 1999 and 2004, respectively. He is a research associate in the Health and Rehabilitation Sciences Research Institute at the University of Ulster. His principal research interests are in the fields of software architecture, digital signal and image processing. Dr. Ritchie is a member of the IEEE Computer Society.

Janice R. Bailie completed a BSc and PhD in Biochemistry at Queen's University Belfast, before taking up a post-doctoral Fellowship in the Department of Ophthalmology at Queen's University Belfast, where her research focused on the molecular biology of the retinal microvasculature. Subsequent appointments included a Fellowship in Radiation Biology and Divisional Molecular Biology Manager in Randox Laboratories Ltd. She is currently working in the Research & Development Office for Health & Social Care. Her research interests are in microvascular gene expression, microvascular endothelial cell biology, angiogenesis and control of microvessel blood flow.

Patricia M. Hart is the Regional Director of Quality Assurance for the Northern Ireland Diabetic Retinopathy Screening Programme, a consultant ophthalmologist a the Royal Victoria Belfast and Honorary Lecturer at Queen's University Belfast. She received a degree in medicine (MB BCh BAO) from Queen's University Belfast in 1975. Post-graduate training and experience were obtained in Belfast, Moorfield's Eye Hospital, London and Singapore National University Hospital, and she has formal training in clinical epidemiology. Areas of special interest and research include medical retinal disease, computer aided and human pattern recognition and prognostic research.